

Experimental and theoretical investigation of the uniform corrosion in the annulus of offshore flexible pipelines.

E. Remita, F. Ropital, J. Kittel, B. Tribollet, E. Sutter, Carol Taravel-Condat, N. Desamais

► **To cite this version:**

E. Remita, F. Ropital, J. Kittel, B. Tribollet, E. Sutter, et al.. Experimental and theoretical investigation of the uniform corrosion in the annulus of offshore flexible pipelines.. Corrosion 2008, Mar 2008, New-Orleans, United States. hal-02475537

HAL Id: hal-02475537

<https://hal-ifp.archives-ouvertes.fr/hal-02475537>

Submitted on 12 Feb 2020

HAL is a multi-disciplinary open access archive for the deposit and dissemination of scientific research documents, whether they are published or not. The documents may come from teaching and research institutions in France or abroad, or from public or private research centers.

L'archive ouverte pluridisciplinaire **HAL**, est destinée au dépôt et à la diffusion de documents scientifiques de niveau recherche, publiés ou non, émanant des établissements d'enseignement et de recherche français ou étrangers, des laboratoires publics ou privés.

EXPERIMENTAL AND THEORETICAL INVESTIGATION OF THE UNIFORM CORROSION IN THE ANNULUS OF OFFSHORE FLEXIBLE PIPELINES

E. Remita, F. Ropital and J. Kittel,
IFP-Lyon,
Rond-point de l'échangeur de Solaize,
BP 3, 69390 Vernaison,
France

B. Tribollet and E. Sutter
Laboratoire Interfaces et Systèmes Electrochimiques, UPR15 du CNRS,
case 133, 4 place Jussieu,
75252 Paris Cedex 05, France

C. Taravel-Condat, N. Desamais
Technip,
rue Jean Huré,
76580 Le Trait, France

ABSTRACT

Flexible pipelines used in the offshore industry are composed of steel wires enclosed in an annulus formed by inner and outer thermoplastic sheaths. The CO₂ corrosion of the carbon steel wires located in this annulus occurs within restricted volumes of electrolyte. For instance, the typical V/S ratio between the volume of electrolyte and the exposed steel surface is in the order of 0.03 mL.cm⁻². In such confined environments, corrosion measurements clearly show that the results classically obtained in bulk conditions (infinite electrolyte volume) do not remain valid. Thus, the corrosion rates measured in the annulus conditions are commonly 2 or 3 orders of magnitude lower than those predicted by classical CO₂ corrosion models. Moreover, measured pH is significantly higher than the saturation pH predicted by thermodynamic models such as CORMED. Recently, large progresses have been made in the understanding of the uniform corrosion processes in the annulus of offshore flexible pipelines. These progresses, related to the design of innovative experimental setups, the achievement of an important testing program and the development of new theoretical models are reported in the present paper.

Keywords: CO₂ corrosion, modelling, super-saturation, siderite, flexible pipelines, confined environment

INTRODUCTION

Flexible pipelines have been used for more than thirty years in offshore applications for the transportation of crude oil, gas and water. In comparison with rigid pipes, flexible pipelines are alternative and economically interesting solutions due to their fast and easy laying procedure, their durability and recoverability. These equipments are also particularly resistant to corrosion: corrosion rates as low as a few micrometers per year were experienced in the annulus of offshore flexible pipelines in the presence of dissolved CO_2 ¹. This particular behavior was generally explained by the high confinement of the electrolyte at the surface of the armor steel wires located in the annulus¹⁻⁴. Indeed, the confinement is empirically known to inhibit corrosion by promoting both a pH increase and a blockage of the steel surface by an insulating siderite (FeCO_3) deposit¹⁻⁴.

Even if a large experimental program was led to improve the understanding of this confinement effect, up to now, no theoretical model was available to describe the particular physico-chemistry of the annulus environment. In particular, pH predictions were achieved using thermodynamic models which ignore both the confinement and the supersaturation of the solution contained in the annulus. As a result, this thermodynamic approach led to a clear overestimation of the severity of the annulus conditions as it will be demonstrated in this article.

In this context, the aim of this paper is to focus on the recent progresses in the investigation of the CO_2 uniform corrosion processes (sweet corrosion) occurring in the annulus space of offshore flexible pipelines. Thus, after a brief description of the flexible pipelines, the different procedures developed for the corrosion testing of the steel wires located in the annulus will be detailed and experimental results will be commented. A new kinetic model allowing the calculation of the different physico-chemical parameters of the annulus environment will also be presented. At the end of the paper, model results will be compared to experimental measurements.

FLEXIBLE PIPELINES AND CORROSION PROCESSES IN THE ANNULUS

Flexible pipelines (flowlines or risers) are composed of different unbonded layers of polymers and steels, each layer being designed to resist to specific loadings. From the inside (bore) to the outside, a flexible pipeline is typically composed of the following main layers (Figure 1):

- A carcass made of stainless steel strip which is formed and spiraled into an interlocking shape. This carcass insures the resistance to external crushing.
- An internal thermoplastic pressure sheath which provides a sealing protection toward the bore environment.
- A pressure vault layer made of carbon steel shaped wires (Zeta or Teta) spiraled at short pitch. This layer is designed to resist to internal pressure loads.
- Two or four armor layers made of carbon steel flat wires helicoidally wounded which insure the resistance to tensile loads.
- An external thermoplastic sheath that seals the pipe from outside environment.

Other layer can be added if necessary, like anti-wear tapes between steel layers, thermal isolation layers....

The carbon steel wires are located in a confined volume between the two internal and external thermoplastic sheaths called "annulus" or "annular space" (Figure 1). Different grades of carbon steel wires and low alloyed carbon steel are used containing between 0.1 % C and 0.75 % C. The temperature varies typically from 20°C to 80°C in the annulus,

depending on the operating conditions in the bore and on the thermal properties of the structure.

The annulus may contain different gases such as CH₄, CO₂, H₂S and possibly condensed water or seawater in case of accidental tearing of the outer sheath. It leads to formation of a corrosive environment in contact with carbon steel wires. Schematically the corrosion situation encountered in the annulus can be summarized according to the scheme proposed in Figure 2.

Recently, a permeability model was proposed to calculate the annulus composition. This model takes into account the transport gas properties of the different polymers used as sheaths, the venting system at end fittings, the bore conditions (fluid composition, temperature, pressure), the external conditions (temperature, depth) and the pipe structure^{5,6}. It allows estimating numerous key parameters which affect the corrosion properties of the armour wires located in the annulus such as P_{CO₂}, P_{H₂S} and the temperature.

In addition to these parameters, it was experimentally evidenced that the V/S ratio of the electrolyte volume to the exposed metallic surface was also a major factor affecting the corrosion behavior of steel in confined aqueous environments¹⁻⁴. This confinement effect makes the classical results obtained in bulk conditions (infinite electrolyte volume) not suitable to describe the corrosion processes occurring in the annulus of offshore flexible pipelines. As a consequence, understanding this effect required specifically adapted studies both from an experimental and a theoretical point of view. In the next section, the different experimental devices developed in our laboratories to achieve such corrosion studies are described.

CORROSION TESTING PROCEDURE FOR THE ANNULUS ENVIRONMENT

A large experimental program was conducted in the last ten years by Technip and IFP for the corrosion testing of the armour wires enclosed in the annulus of flexible pipelines. In order to simulate the annulus environment different devices such as the specifically designed macrocells (Figure 3) and microcells (Figure 4) were used¹. Full scale experiments³ were also recently performed in a real pipeline segment (Figure 5). More classical autoclave tests were also performed in order to work at pressure higher than 1 bar.

Macrocells are basically achieved by placing a large number of steel weight loss specimens in a conventional electrochemical cell (0.9 liter). These cells also include an electrochemical instrumentation involving a steel working electrode, a counter electrode, a reference and a pH electrode. With this kind of device, the confinement ratio V/S can be set in the range 0.15-5 mL.cm⁻² by adjusting the volume of liquid and the number of metallic samples.

Microcells are based on the same principle as macrocells but they contain a lower electrolyte volume equal to 40 mL. With this kind of cells, only weight loss experiments are performed within the main cell. This main cell is connected to an auxiliary cell, supplied with the same electrolyte, where electrochemical measurements are performed. The use of microcells allows reaching V/S ratio ranged between 0.15 and 5 mL.cm⁻².

Contrarily to macrocells and microcells which are limited to 1 bar in internal pressure, autoclave tests allow working at high pressure (more than 10 bars). Confinement ratios as low as 0.2 mL.cm⁻² could be achieved with this technique by adjusting properly the volume of liquid and the number of metallic samples².

Full scale test were notably performed to investigate the fatigue corrosion resistance of flexible pipelines. With this testing method, the tested pipelines present however both a dynamic and a static zone so that these full scale experiments also provided useful information concerning the uniform corrosion processes occurring in the annulus. Full scale tests are very interesting to investigate the corrosion processes occurring in the real

conditions of the pipe service. Indeed, contrarily to microcells and macrocells tests, these tests allow reaching the reel V/S ratio observed in the annulus of flexible pipelines. Depending on the pipe structure, this ratio is ranged between 0.01 to 0.06 mL.cm⁻² in average (locally a maximum ratio of 0.2 mL.cm⁻² can however be reached).

All the results obtained from the different experimental techniques (macrocells, microcells and full scale tests) are consistent and indicate the same tendencies. In confined environments, they first strongly demonstrated that the corrosion behaviour of steel differs drastically from the one observed in bulk conditions (infinite electrolyte volume) at the same temperature and for the same pressure of acid gas¹⁻⁴. More precisely, they revealed notably that both corrosion rates and pH depend on the thickness of the electrolyte layer covering the steel surface¹. Hence, it was shown that, as the V/S ratio decreases, corrosion rates systematically decrease while during the same time the measured pH increases.

Thus, the CO₂ corrosion rates of steel are radically inhibited by the geometrical confinement of the electrolyte in the annulus conditions¹⁻⁴. At 20°C, Ropital *et al.*¹ evidenced, as an example, that CO₂ corrosion rates of low alloyed steel immersed in an electrolyte saturated with CO₂ (P_{CO2} = 1 bar) could be reduced from 2 mm/year to about 5 µm/year when the V/S ratio diminishes from 100 to 0.25 mL.cm⁻². More generally, laboratory measurements^{1,2,4} show that the corrosion rates in confined environments such as the annulus are commonly 2 or 3 orders of magnitude lower than those predicted by the classical CO₂ corrosion models⁷⁻¹¹. Results from full scale experiments³ and the durability of the flexible pipelines currently in service all over the world provide some additional strong evidences of the weakness of the corrosion rates in the annulus of offshore flexible pipelines.

Available studies¹⁻⁴ also report that the very low corrosion rates observed in the annulus are coupled with high values of pH. Hence, the measured pH can sometimes exceed by 1 unit the saturation pH calculated from thermodynamic models such as CORMED which fit experiments only for very large V/S ratios^{1,2,12,13}. For instance, under 1 bar of CO₂ at 20°C, the pH measured for V/S lower than 1,4 mL.cm² are above 6 while the saturation pH predicted by CORMED is equal to 5.3^{1,2}. At higher temperatures (ranged between 50 and 80°) and higher CO₂ partial pressures (ranged between 1.5 to 6.5 bars), a similar behaviour was observed during a full scale test³: pH ranged between 5.2 and 6.3 were measured while CORMED saturation pH ranged between 4.5 and 4.9 were predicted in the same conditions. Furthermore, as already mentioned previously, in such confined corrosive environments, it was also shown that the pH increases as the V/S ratio decreases^{1,2}.

The high values of pH observed in the annulus are generally explained qualitatively by the Fe(II) super-saturation of the solution confined in this space^{1-4,14-16}. The occurrence of this super-saturation state and the empirical dependence between pH and V/S ratio are totally unpredicted by thermodynamics^{12,13}. These two important points clearly underline that the use of a simple thermodynamic description is not well adapted to the case of confined environments such as the annulus.

In fact, thermodynamic models and classical CO₂ corrosion models⁷⁻¹³ were developed on the basis of bulk hypothesis (infinite electrolyte volume) and do not take into consideration the specificities of the mass transport in confined aqueous environments (accumulation of corrosion products, low concentration gradients). This inadequacy between the situations described (confinement) and the hypotheses retained (bulk) can explain the discrepancy between model predictions⁷⁻¹³ and measurements at low V/S.

To overcome such discrepancy, Song *et al.* have recently proposed a model specifically adapted for CO₂ corrosion of steel under a thin liquid layer^{17,18}. The local approach used by these authors leads however to somewhat complicated numerical

calculations. Moreover, by assuming that thermodynamic equilibrium is achieved in the liquid film, Song's model fails to predict the supersaturation phenomena which are classically observed during CO₂ corrosion¹⁵.

Nesic's group also studied the corrosion of steel covered by thin condensation films exposed to CO₂¹⁹. Contrary to Song's approach, their model takes into account the blocking nature of the siderite precipitates formed at the steel surface during corrosion²⁰⁻²². Nevertheless, in thin electrolyte film conditions, their work focused specifically on corrosion rate predictions with no indication concerning pH¹⁹.

Thus, to our best knowledge, the general mechanism which links V/S ratio, P_{CO₂}, θ (coverage ratio of the steel surface by an insulating deposit), pH, and corrosion rate in confined aqueous environments still remains unclear. In this context, a new kinetic model adapted for the CO₂ corrosion occurring in the confined environment of the flexible pipe annulus was developed recently. This model is presenting in the next section of this paper.

CO₂ CORROSION MODEL FOR THE ANNULUS ENVIRONMENT

The simplified geometry of the annulus considered in the model is described in Figure 6. In the present version of the model, only the case of sweet corrosion is considered so that CO₂ is the only acid gas supposed to be present in the annulus.

The seven physico-chemical processes taken into account and reported in Table 1 are the following: the two heterogeneous electrochemical reactions occurring during the corrosion of steel ((I) and (II)), the homogeneous dissociations of dissolved CO₂ ((V) and (VI)) and water (VII), the heterogeneous siderite precipitation (III), and the heterogeneous dissolution of CO₂ (IV). The water dissociation reaction is assumed to be fast enough to be at thermodynamic equilibrium ($K_e = 10^{-20} \text{ mol}^2 \cdot \text{cm}^{-6}$). Such equilibrium hypothesis is not made for the other processes considered.

Due to the possible precipitation of siderite (FeCO₃)^{1,19-22} and due to the eventual presence of grease on the armour steel wires, the steel surface could be partially blocked by an insulating film in the annulus. Thus, a parameter θ (dimensionless) corresponding to the coverage ratio of the surface by such insulating films will be used in the present paper.

Under thin electrolyte layer conditions (as encountered in the annulus of offshore flexible pipelines), experience shows that uniform corrosion rates are low^{1,4}. In such context, it is assumed that the rates of interfacial processes are not limited by mass transport. Then, the concentrations of dissolved species will be supposed homogeneous in the liquid film and heterogeneous reaction rates (processes I, II, IV) will be converted into homogenous production rates (see Table 1) according to relation (1):

$$N_i = j_i \cdot (S/V) \quad (1)$$

With N_i homogenous production rate of the heterogeneous reaction i ($\text{mol} \cdot \text{s}^{-1} \cdot \text{cm}^{-3}$)

j_i rate of the heterogeneous reaction i ($\text{mol} \cdot \text{s}^{-1} \cdot \text{cm}^{-2}$)

S/V ratio between the exposed metallic surface and the liquid volume (cm^{-1})

The steady state is supposed to be achieved. Under this assumption, the concentrations of dissolved species do not depend on time so that the following relations (2) are verified:

$$\frac{\partial c_{Fe^{2+}}}{\partial t} = \frac{\partial c_{H^+}}{\partial t} = \frac{\partial c_{CO_2(aq)}}{\partial t} = \frac{\partial c_{HCO_3^-}}{\partial t} = \frac{\partial c_{CO_3^{2-}}}{\partial t} = 0 \quad (2)$$

Using (1) and the homogeneous production rates as defined in Table 1, relations (2) can be written more explicitly:

$$\frac{S}{V} \cdot \frac{i_{corr}}{2 \cdot F} = N_a = \frac{1}{2} \cdot N_c = N_{prec} = N_{diss} = N_{ac_1} = N_{ac_2} \quad (3)$$

with i_{corr} the corrosion current density ($A \cdot cm^{-2}$)
 F the Faraday constant (96500 C mol^{-1})
 N_i the homogeneous production rate of reaction i ($mol \cdot s^{-1} \cdot cm^{-3}$; see table 1)

Otherwise, the charge balance in the solution and the water dissociation equilibrium are expressed as:

$$2 \cdot c_{Fe^{2+}} + c_{H^+} = c_{HCO_3^-} + c_{OH^-} + 2 \cdot c_{CO_3^{2-}} \quad (4)$$

$$K_e = c_{OH^-} \cdot c_{H^+} \quad (5)$$

Finally, from the set of eight equations constituted by (3), (4), and (5), the six unknown concentrations, the corrosion rate i_{corr} , and the corrosion potential E_{corr} (i.e. rest potential of the steel where $i_{corr} = i_a = i_c$) could be easily calculated in the annulus as a function of V/S , P_{CO_2} and θ at the steady state.

MODEL AND EXPERIMENTAL RESULTS

The constants used for the calculations reported in Figures 7 to 12 of this paper were taken from the literature at $20^\circ C$ ^{9,12,13,16,20,24-29}. Calculated concentrations (pH and Fe^{2+}) were compared to the values returned in the same conditions by the commercial model CORMED (version 2) which assumes that thermodynamic equilibrium is achieved within the liquid phase^{12,13}. This latter assumption is in fact equivalent to consider an infinite electrolyte volume.

In order to quantify more clearly the degree of super-saturation of the solution with respect to Fe^{2+} concentration¹³⁻¹⁵, $Fe(II)$ concentration will be discussed in the present article in terms of super-saturation factor (SF_{Fe}) as defined by relation (6).

$$SF_{Fe} = \frac{c_{Fe^{2+}}}{[c_{Fe^{2+}}]_{eq}} \quad (6)$$

where $[c_{Fe^{2+}}]_{eq}$ is the concentration of Fe(II) at the thermodynamic equilibrium

The influence of the V/S ratio was first investigated for different θ values. A particular attention was paid to the limiting case $\theta = 0$, corresponding to a totally active steel surface, and $\theta = 1$, corresponding to a totally blocked surface (*i.e.* no interfacial flux which implies the achievement of the thermodynamic equilibrium). Results obtained with a CO₂ partial pressure of 1 bar are presented in Figures 7 to 9.

In agreement with experience, the pH value, the Fe(II) concentration, and the corrosion rates calculated from the model vary with the V/S ratio (Figures 7 to 9). Hence, for P_{CO₂} = 1 bar, the pH increases from 5.29 in bulk conditions to values higher than 5.8 for V/S ratios inferior to 0.1 cm (Figure 7). In the same trend, as the V/S ratio decreases, SF_{Fe} increases to reach values of the order of 10 for V/S ratios inferior to 0.01 cm (Figure 8). The corrosion rates decrease when V/S ratios decrease. In the case of V/S ratios inferior to 1 cm, the order of magnitude of the predicted corrosion rates is 10 μm/year for 1 bar of CO₂ (Figure 9).

The dependence on the V/S ratio, experimentally observed¹⁻⁴, has never been clearly evidenced by other existing models¹⁷⁻¹⁹ and remains totally unpredicted by thermodynamics. For high V/S ratios, SF_{Fe} and pH tend towards thermodynamic values (Figures 7 and 8), showing that the kinetic model proposed is consistent with the CORMED model (hypothesis adapted for bulk conditions).

In agreement with Ropital's experiments¹, for small V/S ratios, the corrosion rates (Figure 9) remain much lower than those predicted by the bulk corrosion models under the same CO₂ partial pressure (from 0.85 to 3.7 mm/year according to ref. 8 and 11). Moreover, the effect of θ on the corrosion rates is significant in Figures 9 and 11. As already suggested by Vitse *et al.*¹⁹, the comparison between the model predictions and the experimental results¹ shows that the blocking nature of the siderite deposit ($\theta \neq 0$) should be taken into account to avoid an overestimation of the corrosion rates at low V/S.

Calculated pH values are weakly sensitive to the value of θ . Indeed, changing θ from 0 to 0.9 induced a maximum pH change of 0.3 units, in the whole ranges of V/S and P_{CO₂} investigated (see Figures 7, 10 and 12). As a totally blocked surface (*i.e.* $\theta \rightarrow 1$ and $i_{corr} \rightarrow 0$) is reached, the pH values tends towards thermodynamic pH values (see Figures 7 and 10). This is consistent with the definition of a thermodynamic equilibrium state (steady state with all current densities equal to zero). It is however interesting to note that even a very little activity of the steel surface has a large impact on the calculated pH values. Hence, for instance, in the case of a steel surface blocked at 99% (by grease or siderite), under 1 bar of CO₂, the pH still exceed saturation pH from nearly 0.7 unity for a V/S ratio equal to 0.03 cm typical of flexible pipe annulus (see Figure 7).

In the case of a V/S ratio of 0.03 cm, the impact of the CO₂ partial pressure on pH and corrosion rates is depicted respectively in Figures 10 and 11. As expected, when CO₂ partial pressure increases, pH decreases while the corrosion rates increase. Nevertheless, the calculated pH values always remain above the saturation pH predicted by thermodynamics. Accordingly, the corrosion rates stand at levels much lower than those expected in bulk conditions^{8,11}.

In Figure 12, experimental pH data collected from different past studies¹⁻⁴ are compared to the pH predicted by the model. The pH calculated from the model fit well with the experimental pH measured. In confined environments containing pure CO₂ such as the

annulus, Figure 12 illustrates the improvement of the pH predictions provided by the kinetic model proposed in this article in comparison with the pH prediction made using the CORMED saturation pH.

Finally, the kinetic approach used in the model systematically led to the calculation of Fe(II) concentrations and pH values higher than those predicted by thermodynamics (see Figures 7,8,10, and 12). This situation, in agreement with field observations, is a direct consequence of the slow kinetic of the siderite precipitation reaction. Moreover, due to the relatively high pH values observed in the confined environment, the calculated corrosion rates always remain relatively low even for a totally active steel surface ($\theta = 0$). The comparison between the model and the experiments indicates however that the values of θ are higher than 0.5 at 20°C in confined environments containing dissolved CO₂.

CONCLUSION

A global approach combining experimental techniques development, testing and theoretical modeling of the corrosion processes occurring in the confined environment of the annulus of offshore flexible pipelines was proposed. This approach led to an improved understanding of the links existing between pH, corrosion rates, V/S ratio, the blocking ratio of the steel surface, and CO₂ partial pressure in confined aqueous environment. The Fe(II) supersaturation, the low corrosion rates, and the high values of pH usually observed in experiments at low V/S ratio are notably very well predicted by the kinetic model proposed. This model also underlines particularly the weaknesses of the thermodynamic approach when it is used to calculate pH in confined environments such as the annulus. Thus, in the case of pure CO₂ environment, the model particularly points out the pessimistic character of the pH predictions made using the saturation pH calculated from a thermodynamic model.

For practical purposes, the model could be used to estimate quantitatively the pH values, the corrosion rates, and the Fe(II) concentrations in confined environments containing dissolved CO₂ such as the annulus space of flexible pipelines.

Currently, work is in progress to adapt the model to the case of sour corrosion by taking into account the existence of an H₂S partial pressure in the gas phase. The influence of the temperature will also be taken into account in the next version of the model.

REFERENCES

1. F. Ropital, C. Taravel-Condat, J. N. Saas, C. Duret, Eurocorr 2000, London, (2000), paper C014/55,
2. C. Taravel-Condat, N. Desamais, Conference OMAE 2006, Hambourg, (2006), Paper 92394.
3. N. Desamais, C. Taravel-Condat, "Full scale corrosion fatigue testing of a flexible pipe in CO₂ / H₂S environment", Eurocorr 2006, Maastricht, (2006).
4. C. Taravel-Condat, N. Desamais, "Qualification of very high strength carbon steel wires for use in flexible pipes with presence of small amount of H₂S", Eurocorr 2006, Maastricht, (2006).
5. C. Taravel-Condat, M. Guichard, J. Martin, "MOLDI™: A fluid permeability model to calculate the annulus composition in flexible pipes: Validation with medium scale tests and field cases" Conference OMAE 2003, Cancun, June 2003, Paper 37193
6. Z. Benjelloun-Dabagui, J.-C. De Hemptinne, J. Jarrin, J.-M. Leroy, J.-C. Aubry, J.-N. Saas, C. Taravel-Condat "MOLDI™: A fluid permeability model to calculate the annulus composition in flexible pipes ", Oil and Gas Science and Technology 57, (2002), p. 177.
7. C. De Waard, D. E. Milliams, Corrosion 31 (1975) 178.
8. C. De Waard, U. Lotz, D. E. Milliams, Corrosion 47 (1991) 976.
9. S. Netic, J. Postlethwaite, S. Olsen, Corrosion 52 (1996) 280.
10. L. G.S. Gray, B. Anderson, M. J. Danysh, P. R. Tremaine, Corrosion 1989 Conf., New Orleans, (1989), Paper n° 464.
11. Norsok standard M506, rev1, (1998).
12. M. Bonis, Thèse de Docteur Ingénieur, INSA de Lyon, (1982).
13. J.L. Crolet, M. Bonis, Materials Performance 29 n°7 (1990) 81.
14. M. L. Johnson, M. B. Tomson, Corrosion 91 Conf. , Cincinnati, (1991), Paper n° 473.
15. A. Dugstad, Corrosion 92 Conf., Nashville, (1992), Paper n°14.
16. E.W.J. Van Hunnik, B.F.M Pots, E. L. J. A. Hendriksen, Corrosion 96 Conf., Denver, (1996), Paper 6.
17. F.M Song, D. W. Kirk, J. W. Graydon, D.E. Cormack, J. Electrochem. Soc. 149 (2002) B479.
18. F.M Song, D. W. Kirk, J. W. Graydon, D.E. Cormack, Corrosion 60 (2004) 736.
19. F. Vitse, S. Netic, Y. Gunaltun, D. Larrey de Torreben, P. Duchet-Suchaux, Corrosion 59 (2003) 1075.
20. M. Nordsveen, S. Netic, R. Nyborg, A. Stangeland, Corrosion 59 (2003) 443.
21. S. Netic, M. Nordsveen, R. Nyborg, A. Stangeland, Corrosion 59 (2003) 489.
22. S. Netic, K.L.J. Lee, Corrosion 59 (2003) 616.
23. B.R. Linter, G.T. Burstein, Corros. Sci. 41 (1999) 117.
24. M. Frankignoulle, Limnol. Oceanogr. 33 (1988) 313.
25. J.J. Cole, N.F. Caraco, Limnol. Oceanogr. 43 (1998) 697.
26. D. Wolf-Gladrow, U. Riebsell, Marine Chem. 59 (1997) 17.
27. C. Liu, S. Kota, J.M. Zachara, J.K. Fredrickson, C.K. Brinkman, Environ. Sci. Technol. 35 (2001) 2482.
28. C. Jimenez-Lopez, C.S. Romanek, Geochim. Cosmochim. Acta 68 (2004) 557.
29. T. Xu, J.A. Apps, K. Pruess, Chem. Geol. 217 (2005) 295.

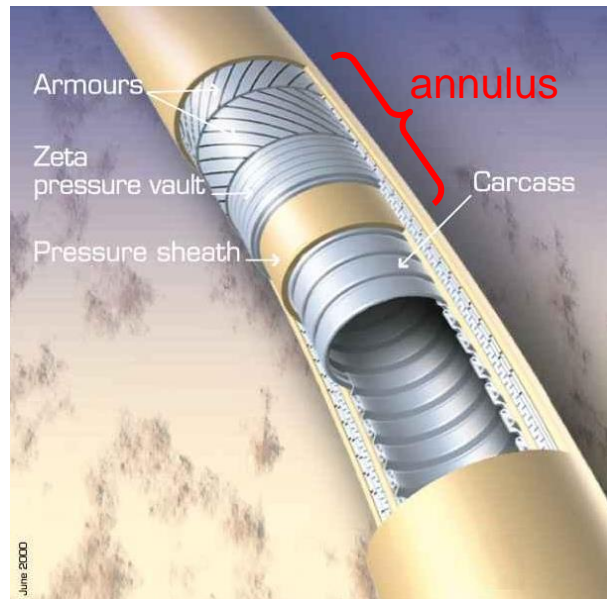


FIGURE 1 - General view of a flexible pipe structure

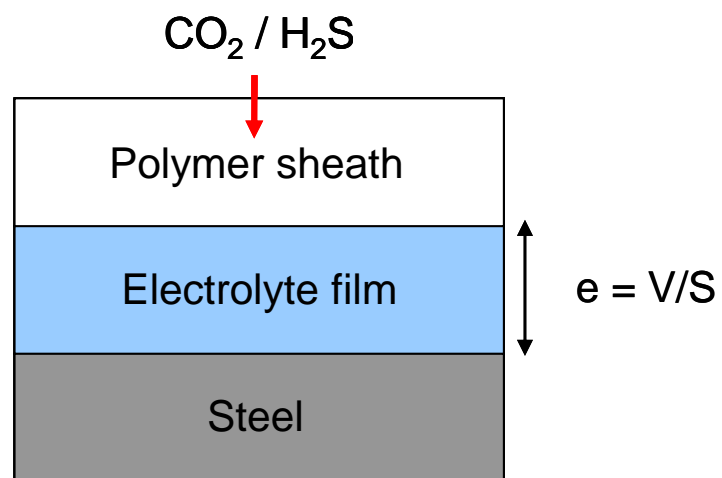


FIGURE 2 – Schematic view of the annulus environment

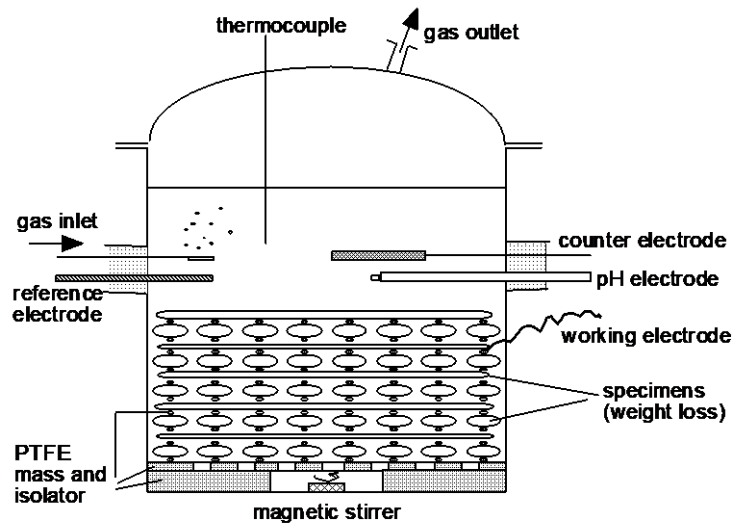


FIGURE 3 – Sketch of a macrocell

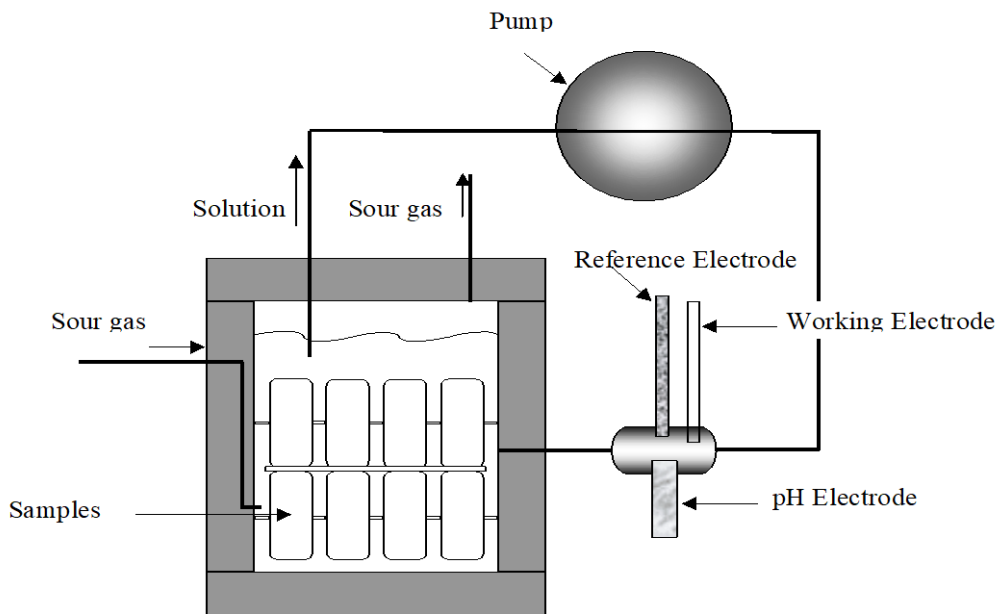


FIGURE 4 – Sketch of a microcell

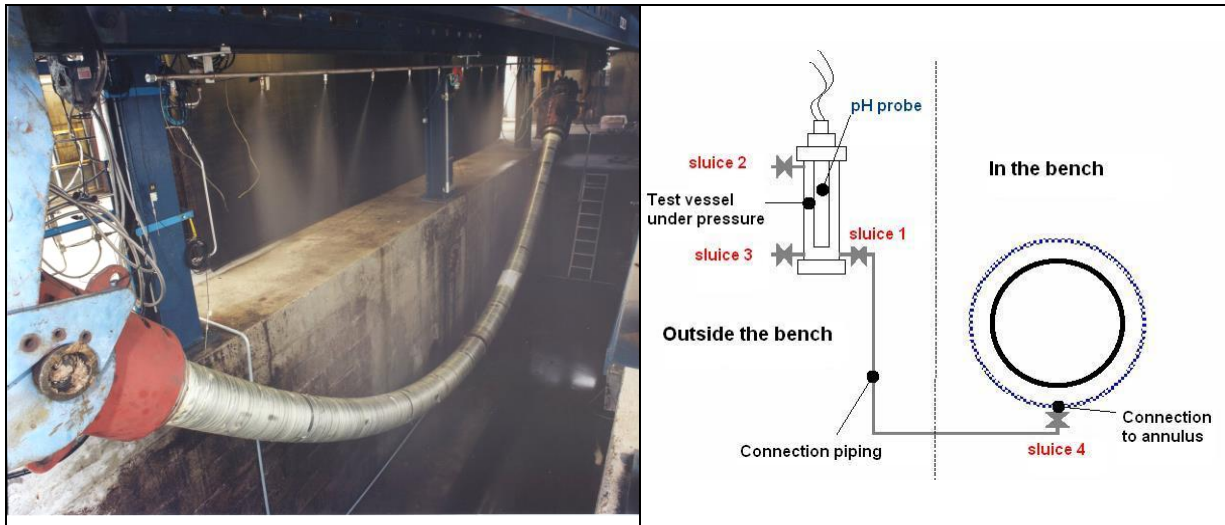


FIGURE 5 – Pipe sample during a full scale fatigue corrosion test and scheme of pH measurements facility

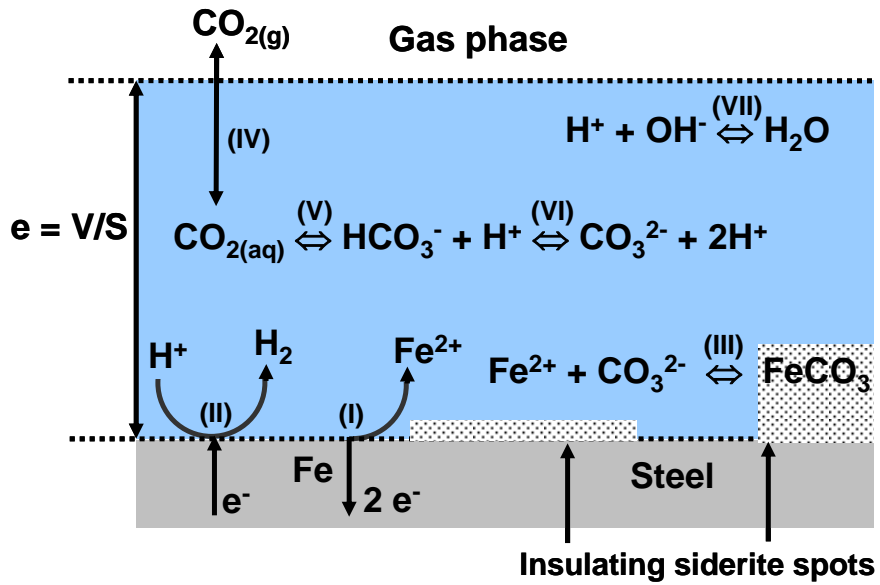


FIGURE 6 – Scheme of the system modeled

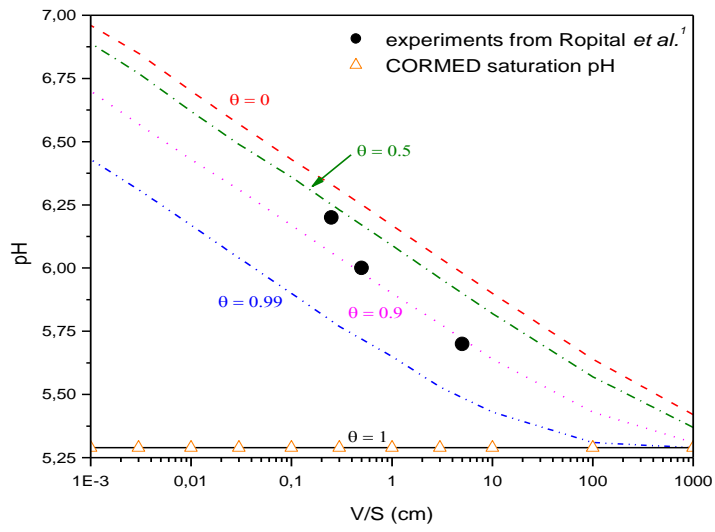


Figure 7 - Evolution of the pH with the V/S ratio for different θ ; $P_{CO_2} = 1$ bar

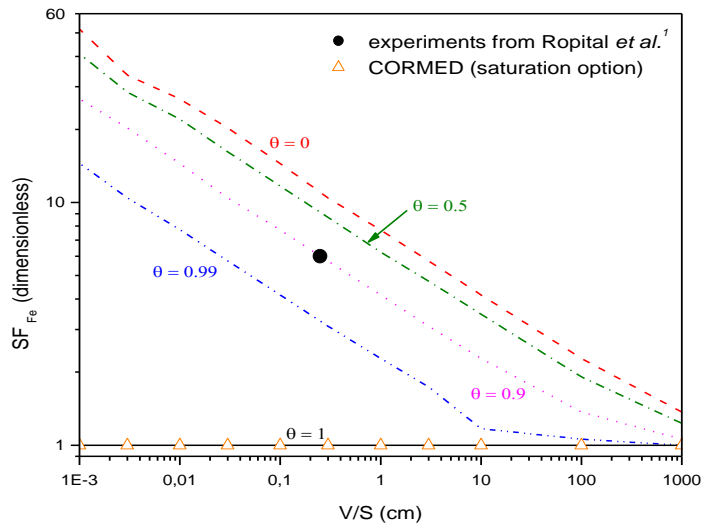


Figure 8 - Evolution of the Fe II sursaturation factor SF_{Fe} with the V/S ratio for different θ ; $P_{CO_2} = 1$ bar

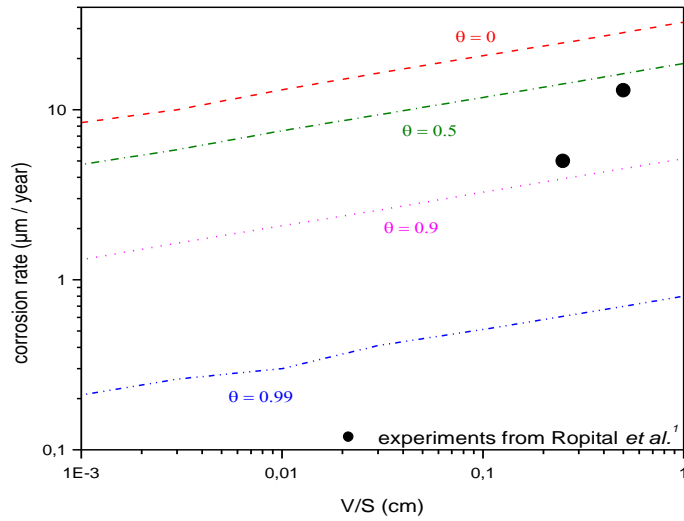


Figure 9 - Evolution of the corrosion rate with the V/S ratio for different θ ; $P_{\text{CO}_2} = 1 \text{ bar}$

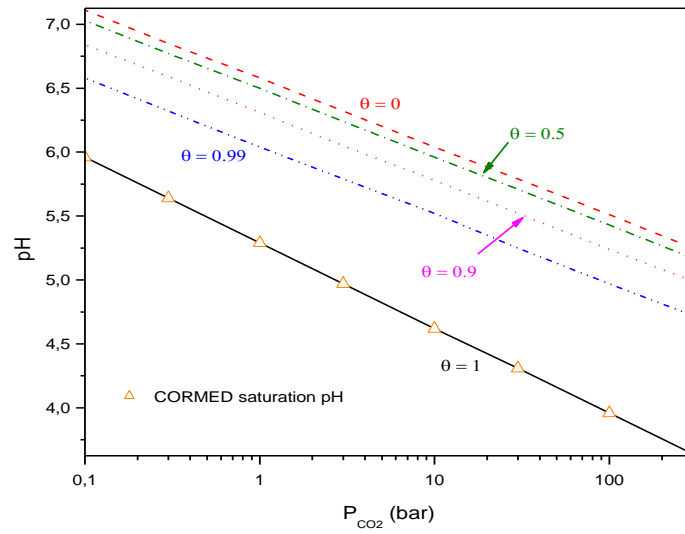


Figure 10 - Evolution of the pH with the CO_2 partial pressure for different θ ; $V/S = 0.03 \text{ cm}$

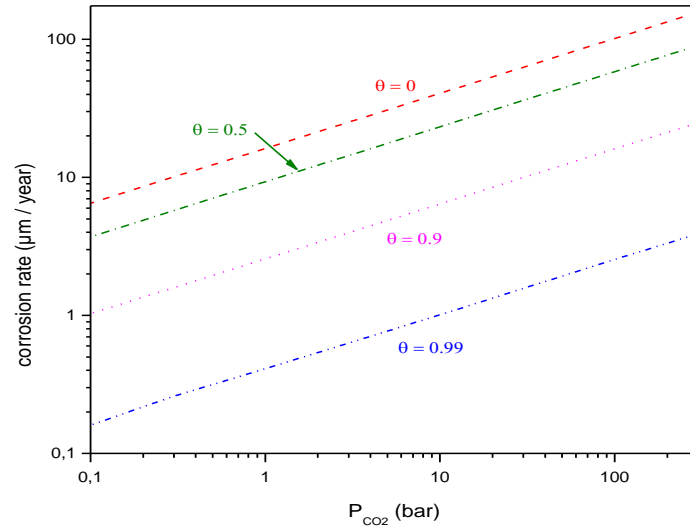


Figure 11 - Evolution of the corrosion rate with the CO₂ partial pressure for different θ ; V/S = 0.03 cm

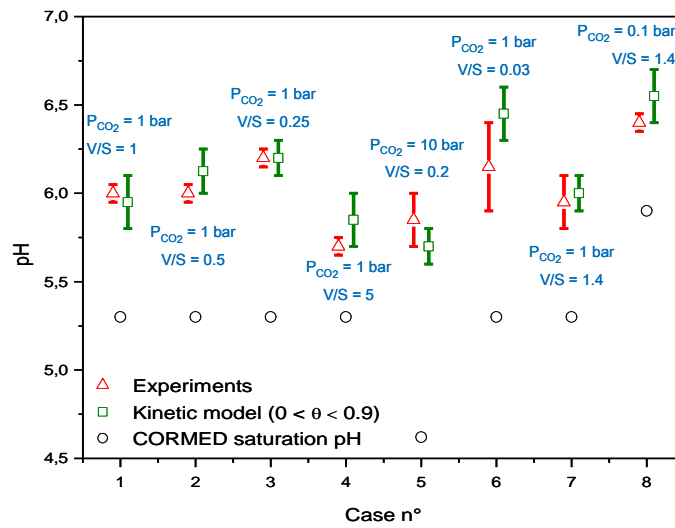


Figure 12 - Comparison between experimental pH¹⁻⁴, pH calculated from our new model and saturation pH calculated from CORMED for different cases taken from the litterature (P_{CO_2} ranged between 0.1 and 10 bar, V/S between 0.03 and 5 mL.cm⁻², 20°C).

Reaction	Reaction equation	Homogeneous production rate (mol.cm ⁻³ .s ⁻¹)	Ref.
Anodic dissolution (I)	$\text{Fe} \rightarrow \text{Fe}^{2+} + 2 \text{e}^-$	$N_a = \frac{S}{V} \cdot \frac{1}{2.F} \cdot (1-\theta) \cdot i_{0_a} \cdot 10^{\frac{E-E_{rev}}{b_a}}$	20
Cathodic reaction (II)	$2 \text{H}^+ + 2 \text{e}^- \rightarrow \text{H}_2$	$N_c = \frac{S}{V} \cdot \frac{1}{F} \cdot (1-\theta) \cdot i_{0_c} \cdot c_{\text{H}^+}^{0.5} \cdot 10^{\frac{E-0.06 \cdot \text{pH}}{b_c}}$	20 23
Siderite precipitation (III)	$\text{Fe}^{2+} + \text{CO}_3^{2-} \leftrightarrow \text{FeCO}_3$	$N_{prec} = k_1 \cdot c_{\text{Fe}^{2+}} \cdot c_{\text{CO}_3^{2-}} - k_{-1}$	16
Gas dissolution (IV)	$\text{CO}_{2(\text{g})} \leftrightarrow \text{CO}_{2(\text{aq})}$	$N_{diss} = \frac{S}{V} \cdot (k_2 \cdot P_{\text{CO}_2} - k_{-2} \cdot c_{\text{CO}_{2(\text{aq})}})$	24 25
First acid dissociation (V)	$\text{CO}_{2(\text{aq})} \leftrightarrow \text{HCO}_3^- + \text{H}^+$	$N_{ac_1} = k_3 \cdot c_{\text{CO}_{2(\text{aq})}} - k_{-3} \cdot c_{\text{H}^+} \cdot c_{\text{HCO}_3^-}$	26
Second acid dissociation (VI)	$\text{HCO}_3^- \leftrightarrow \text{CO}_3^{2-} + \text{H}^+$	$N_{ac_2} = k_4 \cdot c_{\text{HCO}_3^-} - k_{-4} \cdot c_{\text{H}^+} \cdot c_{\text{CO}_3^{2-}}$	26
Water dissociation (VII)	$\text{H}_2\text{O} \leftrightarrow \text{OH}^- + \text{H}^+$	$K_e = c_{\text{OH}^-} \cdot c_{\text{H}^+}$	12

Table 1- Physico-chemical processes considered and corresponding production rates